Optimization of the cylindrical sieves for separating threshed rice mixture using EDEM

Jianbo Yuan[1,2,3], Jufei Wang[3], Hua Li[3*], Xindan Qi[2*], Yongjian Wang[3], Chao Li[3]

(1. *School of Mechanical Engineering, University of Science and Technology Beijing, Beijing 100083, China*;
2. *School of Mechanical and Power Engineering, Nanjing Tech University, Nanjing 211816, China*;
3. *Key Laboratory of Intelligent Agricultural Equipment in Jiangsu Province / Nanjing Agricultural University, Nanjing 210031, China*)

Abstract: The design of the cylindrical sieve equipment used for the screening and separation of agricultural granular materials is mainly through the experimental method, which has the disadvantages of a long development cycle and high cost. To solve this problem, the discrete element method (DEM) was utilized to accurately build the particle models of threshed rice components (grains, shriveled grains, and short stalks), and simulated the separation of grains from the mixture in a cylindrical sieve. The influences of rotational speed (*A*), cylindrical sieve diameter (*B*), cylindrical sieve aperture (*C*), and inclinational angle (*D*) on screening cleaning rate, screening loss rate, and screening efficiency were investigated. Meanwhile, the optimal parameters of the cylindrical sieve were obtained using a central composite design (CCD) under response surface methodology (RSM). The results of CCD showed that the quadratic multinomial model is credible and revealed that the cylindrical sieve aperture has a significant impact on the screening characteristics. It is predicted that the optimal values for screening cleaning rate, loss rate, and efficiency were 97.84%, 0.27%, and 85.38%, respectively, while *A*, *B*, *C*, and *D* were 23.6 r/min, 297 mm, 8.7 mm, and 2 °, respectively. The experimental results using a real threshed rice mixture were found to be in good agreement with the optimal simulation results. This study proved a reliable research method and provides a design reference for the cylinder sieving systems for threshed rice or separation of other bulk material.

Keywords: cylindrical sieve, threshed rice mixture, discrete element method, separation, rice, optimization
DOI: 10.25165/j.ijabe.20221502.5150

Citation: Yuan J B, Wang J F, Li H, Qi X D, Wang Y J, Li C. Optimization of the cylindrical sieves for separating threshed rice mixture using EDEM. Int J Agric & Biol Eng, 2022; 15(2): 236–247.

1 Introduction

China is the largest producer of rice in this world, with a planting area of 3 million km^2, accounting for above 61% of the world's rice production in 2022[1]. The utilization rate of agricultural machinery in China is 79.2% at present, and specialized farming such as mud fields and small plots still rely on human resources for rice cultivation[2]. The process condition of rice harvesting includes cutting, threshing, separation, and transportation, that separation working has a significant impact on the performance of harvesting equipment. Currently, the separation of grains from the threshed rice mixture is accomplished through the planar vibration sieve, yet which cannot meet the requirements under particular conditions. Cylindrical sieve is the equipment mainly encountered in the process of handing and processing granular materials, used in screening process condition of bulk material due to the advantages of relatively simple structure, lighter weight, requiring little operating and low maintenance cost compared to other separation systems[3,4]. In the agriculture domain, the cylindrical sieve is used for the classical bulk material, such as the process of peanut removal and classification, the separation of threshed rice, and threshed rapeseeds[5-8]. The working objects of the cylinder screening equipment are discrete particle groups involving the interaction between particles and particles as well as particles and the sieve[9]. The movement of discrete particle groups in a cylindrical sieve is random with many influencing factors. As such, a variety of methods have been employed by scholars to study particle material screening characteristics in cylindrical sieves. Many early scholar has proposed a theory of particle permeability based on the relationship between particle size and slot dimensions in a cylinder screening system via statistical methods[10,11]. In subsequent studies, some scholars established various mathematical models for studying the motion of particle material separation in a cylindrical sieve and exploring the factors determining the screening effect, which included more abundant discrete materials processing such as municipal solid waste separation, battery screening, and iron tailings[12-14].

Screening is critical in harvesting rice since the field experiments have shown seasonal and higher costs. Cundall[15] proposed a method based on a 2D angular-edge contact discrete element model to analyze the measurement of accelerations in rock slopes for the first time in 1971. This method allows researchers to effectively calculate the motion of discontinuous medium and discrete particle groups. With the development of computer technology, many scholars[16-18] have been able to study the motion processing of bulk materials via the discrete element method.

Received date: 2019-05-15 **Accepted date:** 2022-01-26
Biographies: Jianbo Yuan, PhD candidate, research interests: modern agricultural machinery equipment, Email: 335943408@qq.com; **Jufei Wang**, PhD candidate, research interests: agricultural mechanization and biomass energy, Email: 2020212005@stu.njau.edu.cn; **Yongjian Wang**, Associate Professor, research interests: modern agricultural machinery equipment, Email: yjwang@njau.edu.cn; **Chao Li**, PhD candidate, research interests: agricultural mechanization and biomass energy, Email: 1602726464@qq.com.
***Corresponding author: Hua Li**, PhD, Professor, research interests: agricultural mechanization and biomass energy. Nanjing Agricultural University, Nanjing 210031, China. Tel: +86-13951740692, Email: lihua@njau.edu.cn; **Xindan Qi**, Associate Professor, research interests: modern agricultural machinery equipment. Nanjing Tech University, Nanjing 211816, China. Tel: +86-13552925758, Email: 1710863381@qq.com.

Alchikh-Sulaiman et al.[19] researched the mixing of monodisperse, bidisperse, tridisperse, and polydisperse solid particles in a rotary drum using the discrete element method. Ma et al.[20] established the mathematics models of rice and simulated the dynamic behavior of the binary mixed system (rice and straws) under horizontal vibration by the discrete element method. Xu et al.[21] established mathematics models of different rapeseed threshed outputs components in the EDEM software and obtained the corresponding collision signal characteristic for different components laying the foundation for the design of a signal processing circuit. Wang et al.[22] developed mathematical models of soil-tool interactions to research the effect of soil particle size on soil disturbance behaviors and cutting forces by the discrete element method. However, they simulate the process of discrete particle groups by pure sphere particles or larger appearance deviation and ignore the effect of particle shape on the interaction between particles and particles.

This study presents a numerical simulation for the separation of grains from the threshed rice mixture by EDEM software, allowing for the construction of accurate particle models of components (grains, shriveled grains, and short stalks) by the Multi-Sphere Method (MSM) while and analyzing the influence of cylindrical sieve rotational speed, diameter, aperture, and inclinational angle on screening effect. Besides the objective of this study was to determine optimum working parameters, for achieving maximum screening efficiency and cleaning rate as well as minimum screening loss rate, using a central composite design (CCD) method under response surface methodology (RSM), that allow for the study of different influencing factors on optimization and interactions, as well as quantify their influences on one or more properties of interest within multivariate models[23].

2 Discrete element method

Ground-breaking research on DEM modeling was initially carried out by Cundall and Strack[24] to model the behavior of dense solid assemblies in soil mechanics. In this work, the softball contact model by a modified discrete element method (MDEM) was adopted. The interparticle contact model, as shown in Figure 1, is composed of spring and dashpot, which correspond to the elastic and plastic nature of particles in the normal direction, respectively. In the tangential direction, the model consists of the slider, spring, and dashpot. The governing equations for a particle i interacting with another particle j can be written as[25,26].

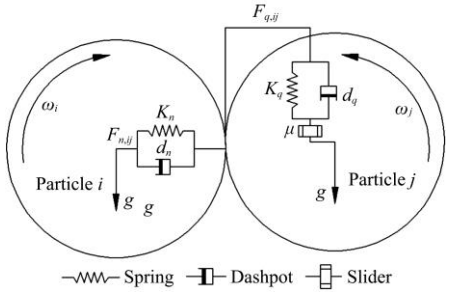

Note: k_n is the normal stiffness coefficient; d_n is the normal damping coefficient; k_q is the tangential stiffness coefficient; d_q is the tangential damping coefficient; μ is the sliding friction coefficient; ω_i is the angular velocity of the particle i, r/min; g is the gravitational acceleration, kg/m^2; $F_{n,ij}$ is the normal force, N; $F_{q,ij}$ is the tangential force N.

Figure 1 Softball contact model of discrete element method

$$m_i \cdot \frac{\mathrm{d}v_i}{\mathrm{d}t} = m_i g + \sum_{j=1}^{n_i} (F_{n,ij} + F_{q,ij}) \tag{1}$$

$$I_i \cdot \frac{\mathrm{d}\omega_i}{\mathrm{d}t} = \sum_{j=1}^{n_i} (T_{q,ij} + T_{r,ij}) \tag{2}$$

where, m_i (kg) v_i (m/s), and ω_i (r/min) are the mass, translational velocity, and angular velocity of the particle i, respectively; g is the gravitational acceleration, kg/m^2; I_i is the moment of inertia of the particle i, kg·m^2; The normal force $F_{N,ij}$ (N), the tangential force $F_{q,ij}$ (N), the rolling torque $T_{r,ij}$ (Nm), and the rolling friction torque $T_{R,ij}$ (Nm) can be obtained by using the basic Newtonian Mechanics Formula, also, each particle simultaneously moves and rolls under the action of the above forces and moments[27,28].

$$F_{n,ij} = k_n \delta_{n,ij} + c_n \delta_{n,ij} \tag{3}$$

$$F_{q,ij} = \min\left\{ k_q \delta_{q,ij} + c_q \delta_{q,ij}, \mu F_{n,ij} \frac{\delta_{q,ij}}{|\delta_{q,ij}|} \right\} \tag{4}$$

$$T_{q,ij} = R_i \cdot F_{q,ij} \tag{5}$$

$$T_{r,ij} = -\mu_r |F_{n,ij}| \frac{\omega_i}{|\omega_i|} \tag{6}$$

where, k_n, k_q, c_n, and c_q are the normal stiffness coefficient, tangential stiffness coefficient, normal damping coefficient, and tangential damping coefficient, respectively; $\delta_{n,ij}$ and $\delta_{q,ij}$ are the normal overlap and the tangential overlap between particles i with j, m; μ and μ_P are the coefficients of sliding friction and the coefficient of rolling friction, respectively; R_i is the radius of the particle i, mm.

3 Materials and methods

3.1 3D model of cylindrical sieve

The 3D models of cylindrical sieve were established based on the single factor simulation conditions described in Section 3.3.1. The intervals of cylindrical sieve holes and cylindrical sieve length were 3 mm (such as size a) and 750 mm, respectively, as shown in Figure 2.

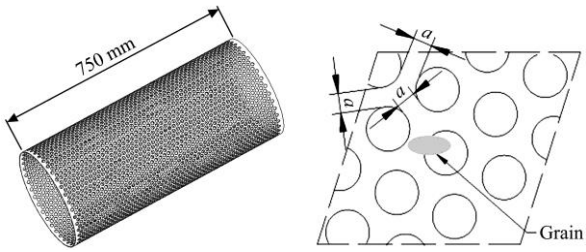

a. Cylindrical sieve length b. Intervals of cylindrical sieve holes

Note: a is the hole spacing of the cylindrical sieve, m.

Figure 2 3D model of cylindrical sieve of this study

3.2 3D particle models of threshed rice components

The study subject herein was Late Rice Nanjing No. 9108 produced in Southern China. The grain, shriveled grain, and short stalks were determined by statistics, with the moisture content be of 14.63%, 8.27%, and 4.44%, respectively. The 3D point cloud data of components were obtained by using a 3D laser scanning system[29]. The 3D CAD models of components were reconstructed and compared with the actual size of the components, errors relating to length, width, thickness, and volume were within 5%, as can be seen in Table 1 and Figures 3a-3c. The components particle models were constructed using the Multi-Sphere Method (MSM) fast filling method, as shown in Figures 3d-3f[30,31]. The number of spheres of grain, shriveled, and short stalk is 336, 410, and 18, respectively, with errors relating to length, width, thickness, and volume were within 5%. In addition, the accuracy of the particle model was higher than that of previous results[17,32].

Table 1 Comparative analysis of the size of rice particle model, 3D model, and actual rice

Components	Dimension	Actual rice/mm	3D model/mm	Error/%	Actual rice/mm	Particle model/mm	Error/%
Grain	Length	6.70	6.65	0.75	6.70	6.45	3.73
	Width	3.35	3.25	2.99	3.35	3.20	4.48
	Thickness	2.25	2.20	2.22	2.25	2.16	4.00
Shriveled grain	Length	7.30	7.20	1.37	7.30	7.16	1.92
	Width	3.35	3.50	4.48	3.35	3.42	2.09
	Thickness	1.57	1.60	1.91	1.57	1.64	4.46
Short stalk	Length	38.00	37.00	2.63	38.00	36.5	3.95
	Diameter	2.10	2.20	4.76	2.10	2.20	4.76

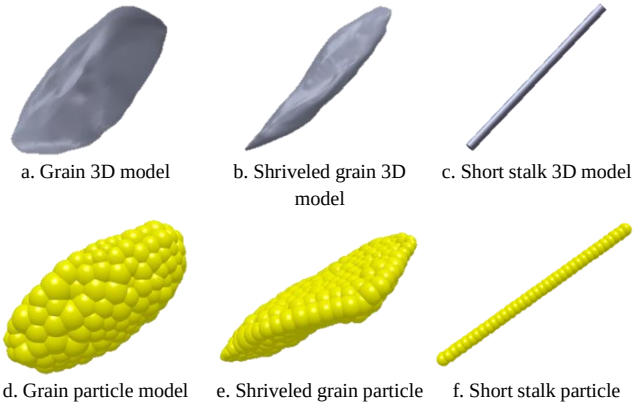

a. Grain 3D model b. Shriveled grain 3D model c. Short stalk 3D model

d. Grain particle model e. Shriveled grain particle model f. Short stalk particle model

Figure 3 3D and particle models of threshed rice components

3.3 Simulation detail setting

The quality ratios of threshed rice mixture, including grains, shriveled grains, and short stalks were 91.24%, 6.23%, and 2.53%, respectively. This work identified the total simulation time as 2.2 s, considering the effect of simulation and numerical computation. The fixed time step t=5×10^{-6} s. To meet the requirements of micro-small harvesting machinery for complex cultivated land in China[33]. Particles were loaded from "Particle Factories" at a fixed rate (6863 grains/s (0.329 kg), 1406 shriveled grains/s (0.0297 kg), and 25 short straws/s (0.0019 kg)) with an initial velocity V_0=1 m/s (Experimentally measured data) at the point then they entered into the calculation domain. A diagram of the threshed rice mixture screening by a cylindrical sieve is shown in Figure 4. The physical parameters of components of the threshed rice (as shown in Table 2 and Table 3) were measured[34], in which the Poisson's rate was determined according to Reference [35].

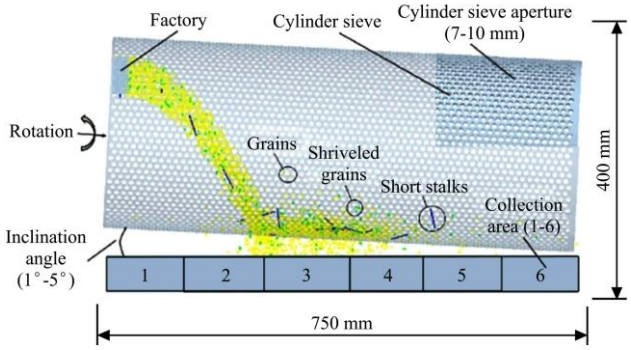

Figure 4 Cylinder screening simulation diagram

Table 2 Physical parameters of the threshed rice components

Object	Poisson's rate	Density/kg m^{-3}	Shear modulus/MPa
Grains	0.30	1256	7.95
Shriveled grains	0.35	309	2.27
Short stalks	0.40	146	0.88
Screen	0.30	7800	7000.00

Table 3 Parameters of physical characteristics of components mutual contact

Object	Coefficient of restitution	Coefficient of static friction	Coefficient of rolling friction
Grains - Grains	0.65	0.65	0.02
Grains - Shriveled grains	0.32	0.64	0.02
Grains - Short stalks	0.31	0.66	0.02
Grains - Sieve	0.53	0.32	0.01
Shriveled grains - Shriveled grains	0.37	0.66	0.02
Shriveled grains - Short stalks	0.36	0.66	0.02
Shriveled grains - Sieve	0.40	0.41	0.01
Short stalks - Short stalks	0.34	0.29	0.02
Short stalks - Sieve	0.28	0.29	0.01

3.3.1 Scheme of single factor simulations

The particle screen-penetrating probability mainly depends on the ratio of the projection, whereby the cross-section of the particle on the sieve and sieve hole, in addition to the size of the particle, is less than 3/4 of the sieve aperture, which is referred to as an "easy to screen particle," as opposed to a "hard to screen particle"[36]. The cylindrical sieve aperture and inclinational angle were determined by the size of the grain, the average length and width of the grains are 6.7 mm and 3.35 mm, respectively, and the experience of the rice harvesting. In summary, the influencing conditions on cylinder screening characteristics were determined to be the aperture, rotational speed, diameter, and inclinational angle of the cylindrical sieve. The single-factor simulation scheme is listed in Table 4.

Table 4 Coupled simulation parameters of single-factor

No.	Factor	Variable's value	Condition
1-5	Cylindrical sieve aperture/mm	7.00, 7.75, 8.50, 9.25, 10.00	26 r min^{-1}, 300 mm, 3 °
6-10	Cylindrical sieve rotational speed/r min^{-1}	21.0, 23.5, 26.0, 28.5, 31.0	8.5 mm, 300 mm, 3 °
11-15	Cylindrical sieve diameter/mm	250, 275, 300, 325, 350	8.5 mm, 26 r min^{-1}, 3 °
16-20	Cylindrical sieve inclinational angle/(°)	1, 2, 3, 4, 5	26 r min^{-1}, 8.5 mm, 300 mm

3.3.2 Scheme of CCD simulations

It was necessary to consider and optimize several factors to obtain the best screening effect. A CCD under RSM was used to reduce the number of simulations, and to investigate the impact and interaction of the various variables by designing simulations. CCD has demonstrated that it is possible to obtain the same conclusions from a reduced number of experiments[37]. The values of cylindrical sieve rotational speed (A), cylindrical sieve diameter (B), cylindrical sieve aperture (C), and cylindrical sieve inclinational angle (D) were determined based on single factor simulation results (Section 4.1). In addition, a CCD in the form of 5^4 factorial simulations was used, as shown in Table 5 and Table 6.

In this model, 30 simulations including six central simulations were selected to minimize the effect of uncontrolled variables, considering the screening cleaning rate, screening loss rate, and screening efficiency as the evaluation index. The influence of critical factors and the model efficiency were verified through ANOVA analysis.

Table 5 Simulations design for conducting the study

No.	Variable	Level 1	Level 2	Level 3	Level 4	Level 5
1	Cylindrical sieve rotational speed (*A*)/r·min^{-1}	21.0	23.5	26.0	28.5	31.0
2	Cylindrical sieve diameter (*B*)/mm	250	275	300	325	350
3	Cylindrical sieve aperture (*C*)/mm	7.00	7.75	8.50	9.25	10.00
4	Cylindrical sieve inclination angle (*D*)/(°)	1	2	3	4	5

Table 6 Results of simulations using CCD

No.	Cylindrical sieve rotational speed (*A*)/r·min^{-1}	Cylindrical sieve diameter (*B*)/mm	Cylindrical sieve aperture(*C*)/mm	Cylindrical sieve inclination angle (*D*)/(°)	Screening cleaning rate/%	Screening loss rate/%	Screening efficiency/%
1	26.0	300	8.50	5	97.97	1.10	82.69
2	28.5	325	7.75	2	97.85	0.95	80.13
3	23.5	325	7.75	2	98.40	0.87	81.66
4	28.5	275	9.25	2	96.27	0.35	84.82
5	26.0	250	8.50	3	98.57	0.35	83.20
6	23.5	275	7.75	4	97.68	1.00	81.61
7	26.0	300	8.50	3	97.97	0.42	83.90
8	21.0	300	8.50	3	97.77	0.35	84.65
9	28.5	275	9.25	4	96.20	0.52	85.49
10	28.5	275	7.75	2	97.57	0.45	80.35
11	26.0	300	8.50	3	97.82	0.30	84.80
12	26.0	300	10.00	3	95.53	0.30	85.20
13	28.5	325	7.75	4	97.48	0.93	79.03
14	23.5	325	9.25	4	96.80	0.56	85.31
15	26.0	300	8.50	3	97.77	0.41	83.50
16	26.0	350	8.50	3	97.87	0.80	83.20
17	26.0	300	8.50	3	97.67	0.37	83.20
18	26.0	300	7.00	3	98.21	0.98	76.85
19	23.5	275	9.25	4	97.29	0.66	83.52
20	26.0	300	8.50	3	97.87	0.38	83.60
21	23.5	325	7.75	4	97.71	0.83	80.74
22	28.5	325	9.25	4	96.40	0.80	86.09
23	23.5	275	9.25	2	96.57	0.31	86.92
24	28.5	275	7.75	4	97.94	0.96	80.73
25	23.5	325	9.25	2	97.31	0.43	86.74
26	31.0	300	8.50	3	96.69	0.76	81.77
27	26.0	300	8.50	3	97.47	0.27	83.70
28	23.5	275	7.75	2	98.81	0.56	79.60
29	26.0	300	8.50	1	97.81	0.28	86.89
30	28.5	325	9.25	2	97.97	1.10	82.69

3.4 Experimental platform

In the experiment platform, the proportions of the threshed rice mixture components were in line with the simulations, and the total weight was 1 kg, which was tested on the laboratory test bench, as shown in Figure 5. The procedure can be briefly described as follows: set values of the speed of the conveyor belt, cylindrical sieve rotational speed, and inclinational angle, then start the motor and conveyor belt. The mixture was screened in the cylindrical sieve. After the mixture has fully entered the cylindrical sieve, all power was disconnected. Each component of the undersized mixture was counted in each collection box. The screening efficiency *P*, screening cleaning rate *C*, and screening loss rate *L* were calculated by Equations (7)-(9)[38].

$$P = \frac{m_{gc}}{m} \tag{7}$$

$$C = \frac{m_{gc}}{m_c} \tag{8}$$

$$L = \frac{(m_g - m_{gs} - m_{gc})}{m_g} \tag{9}$$

where, m is the mass of the threshed rice mixture, kg; m_g is the mass of the grain, kg; m_{gs} is the mass of the grain in the cylindrical sieve, kg; m_{gc} is the mass of the undersized grains in the collection boxes, kg; m_c is the mass of the undersized mixture in the collection boxes, kg.

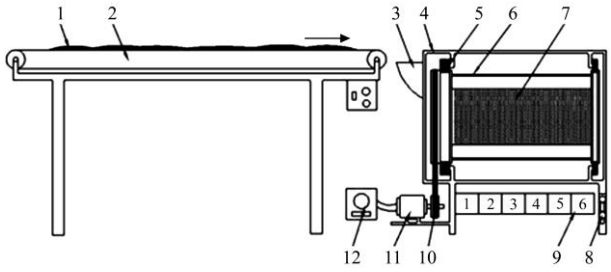

1. Grain 2. Conveyor 3. Feeding inlet 4. Frame 5. Supporting roller 6. Trommel screen bracket 7. Trommel screen 8. Height adjustment 9. Collection box 10. Belt drive 11. Electromotor 12. Univertor

Figure 5 Rice cylindrical screening experimental platform

4 Results and discussion

4.1 Analysis of the single factor simulation results

1) The influence of cylindrical sieve rotational speed on the

screening characteristics

The operation of the cylindrical sieve was mainly based on centrifugal force, whereby a higher rotational speed can allow the cylindrical sieve to work steadily in a tilting state. At the same time, screening efficiency, screening cleaning rate, and screening loss rate were affected. As shown in Figure 6a, a polynomial nonlinear fitting equation and curve are derived and showed that the screening cleaning rate and screening efficiency decreased, and the screening loss rate increased with an increase in the cylindrical sieve's rotational speed. When the rotational speed was lower, the relative velocity of the mixture and the sieve surface was lower. Therefore, the mixture had a higher chance of being screened, and fewer grains fell from the end of the cylindrical sieve, while some of the shriveled grains were sieved to cause a more significant miscellaneous rate. The highest screening efficiency was 84.65%, and the lowest screening loss rate was 0.35% with a cylindrical sieve rotational speed of 21 r/min. The highest screening cleaning rate was 97.82% when the cylindrical sieve rotational speed was 26 r/min.

2) The influence of cylindrical sieve diameter on the screening characteristics

The grains accumulate in the cylindrical sieve and undergo screening, affected by the gravity field, centrifugal force, and friction. Figure 6b shows that the cylindrical sieve diameter had a small influence on the screening loss rate. Moreover, screening efficiency increased and the screening cleaning rate decreased as the cylindrical sieve diameter increased. The lowest screening loss rate was 0.35% when the cylindrical sieve diameter was 250 mm and the highest screening efficiency was 0.35% with a cylindrical sieve diameter of 350 mm. The screening cleaning rate was stable at 97.8%.

3) The influence of cylindrical sieve aperture on the screening characteristics

According to the particle screen-penetrating theory, the larger the aperture is, the easier the mixture screening. Screen aperture clogging occurs when the pore size is small, which leads to lower screening efficiency, although it will increase the screening cleaning rate. Figure 6c shows that a decreasing trend in the screening cleaning rate and screening loss rate, as well as an increasing trend in the screening efficiency, could be observed with an increase in the cylindrical sieve aperture. The highest screening cleaning rate was 98.21% when the cylindrical sieve aperture was 7 mm. The highest screening efficiency and the lowest screening loss rate were 85.20% and 0.30%, respectively, with a cylindrical sieve aperture of 10 mm.

4) The influence of cylindrical sieve inclinational angle on the screening characteristics

The mixture flows along the axis in the sieve under the impact of gravity. The higher the inclinational angle is, the faster the axial flow velocity of the mixture, therefore, the easier the grain is to fall at the end of the cylindrical sieve. As shown in Figure 6d, with an increase in the cylindrical sieve inclination angle, the axial velocity of components also increased so that the residence time of grains in the sieve decreased leading to a reduction in the screening cleaning rate while the screening loss rate markedly increased. This resulted in an increase and then a decrease in the screening efficiency. The highest screening cleaning rate and the lowest screening loss rate were 97.81% and 0.18%, respectively, with a cylindrical sieve inclination angle of 1°. The highest screening efficiency was 85.7% when the cylindrical sieve inclination angle was 2°.

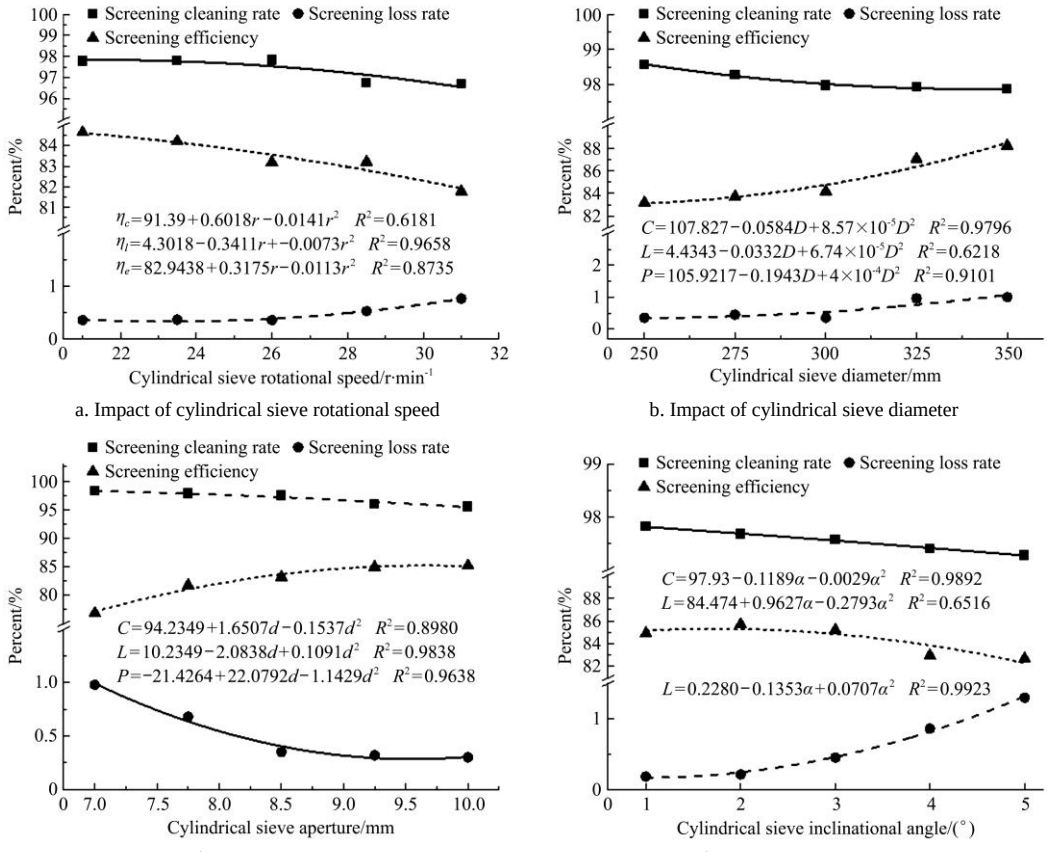

a. Impact of cylindrical sieve rotational speed

b. Impact of cylindrical sieve diameter

c. Impact of cylindrical sieve aperture

d. Impact of cylindrical sieve inclinational angle

Figure 6 Single factor simulation results

4.2 CCD simulation result analysis

4.2.1 CCD simulation result analysis for screening cleaning rate

The adequacy of the statistical model was checked using ANOVA analysis, as can be seen in Table 7 and Figure 7. The

p-value of the model was less than 0.0001, suggesting that the model was strongly significant. The *p*-value of *C* was less than 0.0001, suggesting that it was strongly significant for screening cleaning rate at the linear and quadratic levels; the *p*-value of *A* was less than 0.001, suggesting that it was highly significant for screening cleaning rate; the *p*-value of *B*, *D*, *AB*, *AC*, *AD*, *BC*, *BD*, and *CD* was greater than 0.05, suggesting that *B*, *D* and between any two independent variables were not significant for screening cleaning rate. According to the *F*-value of the various factors shown, it can be seen that the effect of various factors on the screening cleaning rate in descending order of *C*, *A*, *D* and *B* within the test conditions. Furthermore, the cylindrical sieve aperture was the main influencing factor in the screening cleaning rate. The analysis results of ANOVA for the response surface quadratic statistic model were represented. A multiple-order polynomial optimum equation for screening cleaning rate η_C was derived as Equation (10).

$$\eta_C = 92.96 + 1.46A + 6.52C - 0.028A^2 - 0.475C^2 \quad (10)$$

The R^2 was calculated as 0.91 for the screening cleaning rate, indicating a strong agreement between the experimental and predicted values. The *Adj*-R^2 was 0.83, as the mixture movement was random in the cylindrical sieve. The *CV* was 0.32%, suggesting that the experiment was highly reliable. The *p*-value of the "Lack of fit" was greater than 0.005, suggesting that it was not significant. The model was found to be adequate for making predictions within the range of variables employed.

Table 7 ANOVA for response surface quadratic model

Source	Sum of squares	df	Mean square	*F*-value	*p*-value	Significance
Model	15.870	14	1.130	11.340	<0.0001	***
A	1.870	1	1.870	18.700	0.0006	**
B	0.089	1	0.089	0.890	0.3609	
C	10.190	1	10.190	101.900	<0.0001	***
D	0.068	1	0.068	0.680	0.4217	
AB	2.5×10^{-3}	1	2.5×10^{-3}	0.025	0.8765	
AC	0.065	1	0.065	0.650	0.4327	
AD	0.160	1	0.160	1.640	0.2198	
BC	0.070	1	0.070	0.700	0.4152	
BD	0.120	1	0.120	1.190	0.2925	
CD	0.260	1	0.260	2.600	0.1277	
A^2	0.860	1	0.860	8.600	0.0103	**
B^2	0.140	1	0.140	1.360	0.2618	
C^2	1.960	1	1.960	19.560	0.0005	**
D^2	0.004	1	0.004	0.040	0.8841	
Residual	1.500	15	0.010			
Lack of fit	1.350	10	0.013	4.430	0.0570	
Pure error	0.015	5	0.030			
Total error	17.370	29				

Note: *** Strongly significant (p<0.001); ** Highly significant (p<0.01); * Significant (p<0.05). df is the degree of freedom.

Cylindrical sieve rotational speed (*A*) and cylindrical sieve diameter (*B*)

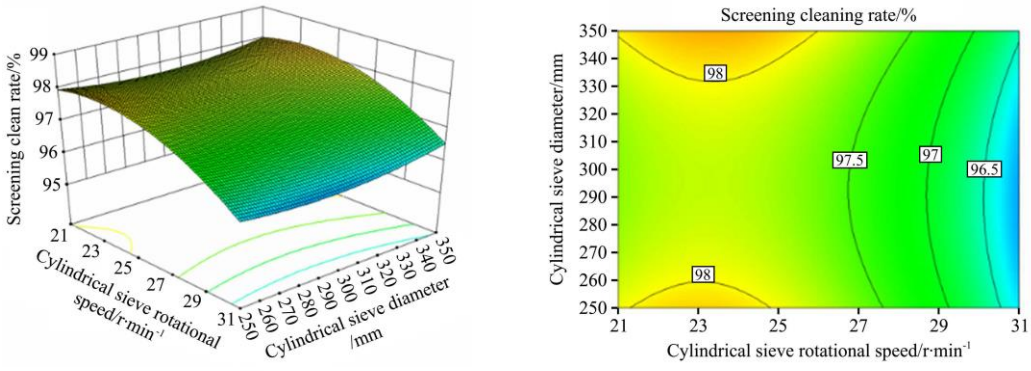

Cylindrical sieve rotational speed (*A*) and cylindrical sieve aperture (*C*)

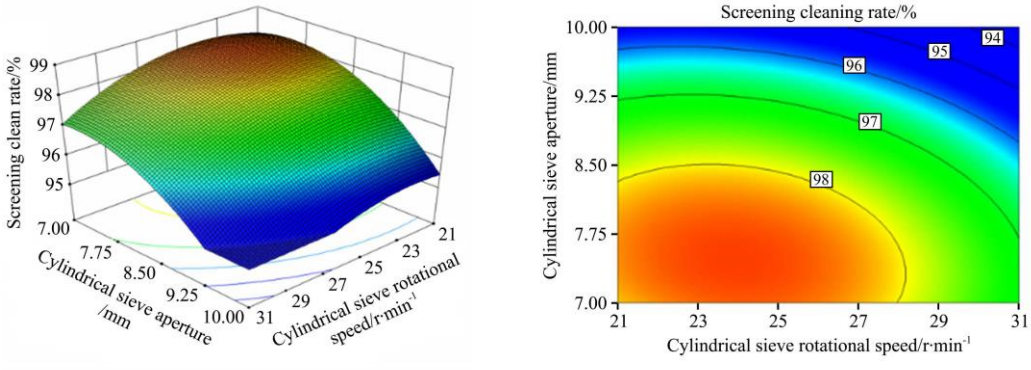

Cylindrical sieve rotational speed (*A*) and cylindrical sieve inclination angle (*D*)

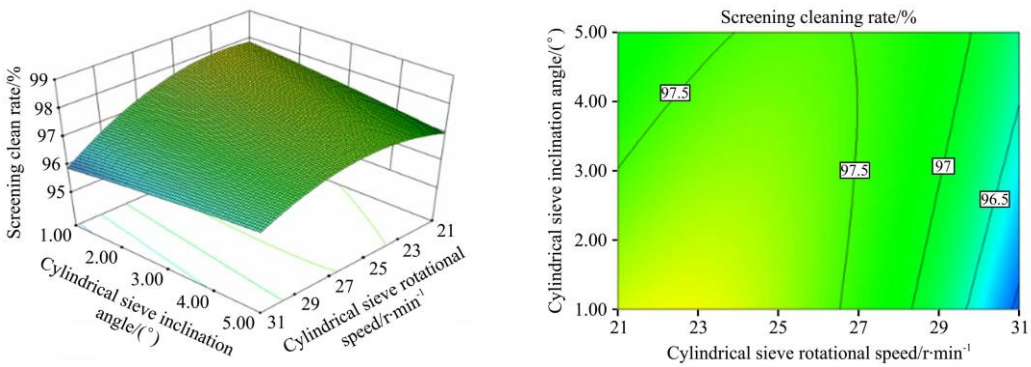

Cylindrical sieve diameter (*B*) and cylindrical sieve aperture (*C*)

Cylindrical sieve diameter (*B*) and cylindrical sieve inclination angle (*D*)

Cylindrical sieve aperture (*C*) and cylinder inclination angle (*D*)

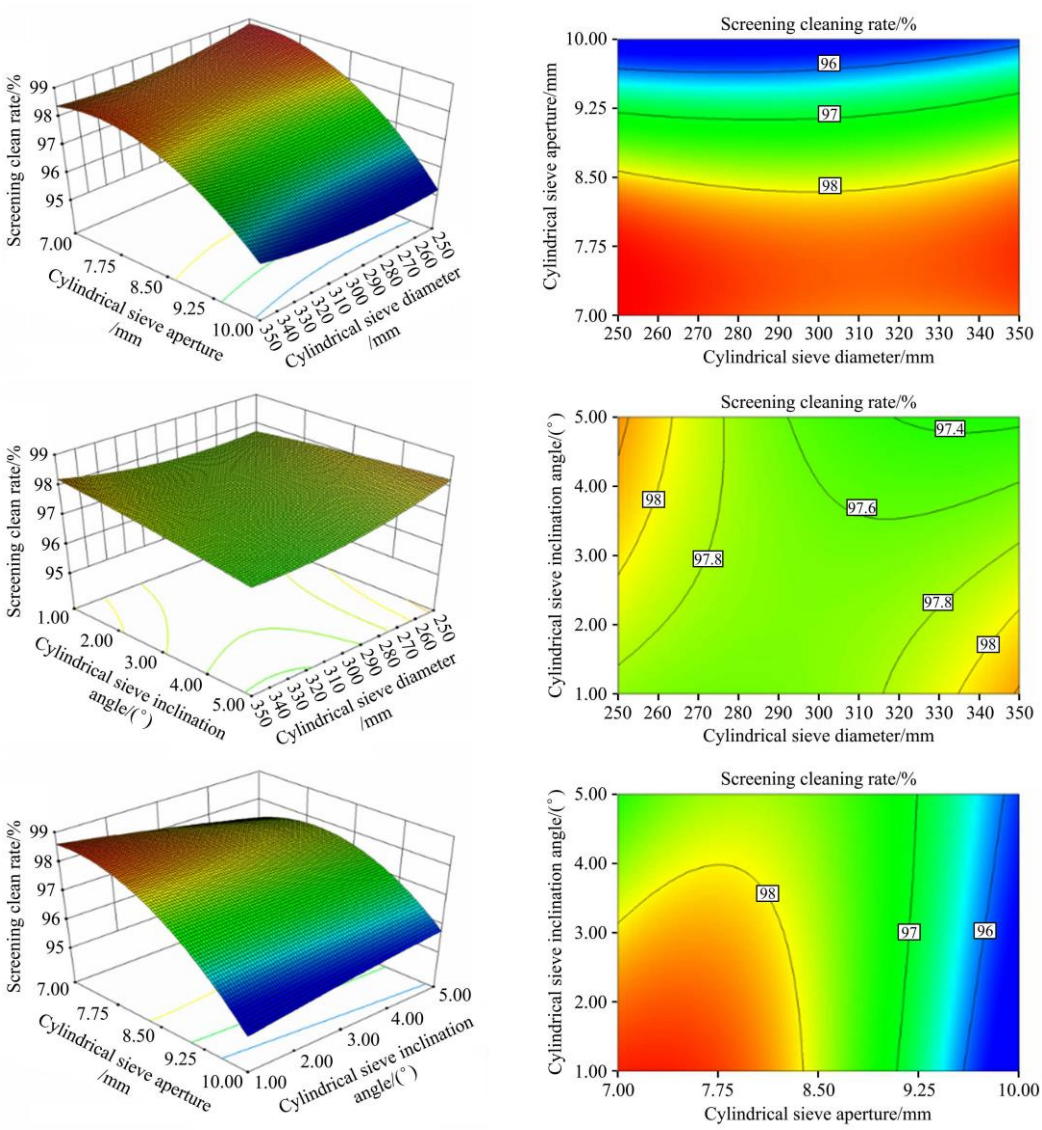

a. 3D response surface plots b. 2D contour plots

Figure 7 3D response surface plots and 2D contour plots for screening cleaning rate

4.2.2 CCD simulation result analysis for screening loss rate

The adequacy of the model was checked using ANOVA analysis, as shown in Table 8. The *p*-value of the model was less than 0.0001, suggesting that the model was strongly significant. The *p*-value of *C* and *D* was less than 0.0001, suggesting that it was strongly significant for screening loss rate; the *p*-value of *B* was less than 0.001, suggesting that it was highly significant for screening loss rate; the *p*-value of *BD* was less than 0.05 suggesting that it was significant for screening loss rate (Figure 8), and the *p*-value of *A*, *AB*, *AC*, *AD*, *BC*, and *CD* were greater than 0.05 suggesting that it was no significance for screening loss rate.

Table 8 ANOVA for response surface quadratic model

Source	Sum of squares	df	Mean square	*F*-value	*p*-value	Significance	Source	Sum of squares	df	Mean square	*F*-value	*p*-value	Significance
model	1.860	14	0.130	10.830	<0.0001	***	*CD*	7.56×10^{-4}	1	7.56×10^{-4}	0.062	0.8075	
A	0.063	1	0.063	5.130	0.0388	*	A^2	0.098	1	0.098	7.950	0.0129	*
B	0.190	1	0.190	15.380	0.0014	**	B^2	0.110	1	0.110	9.340	0.0080	**
C	0.540	1	0.540	44.170	<0.0001	***	C^2	0.180	1	0.180	14.620	0.0017	*
D	0.460	1	0.460	37.130	<0.0001	***	D^2	0.240	1	0.240	19.480	0.0005	**
AB	0.052	1	0.052	4.210	0.0581		Residual	0.180	15	0.012			
AC	7.66×10^{-3}	1	7.66×10^{-3}	0.620	0.4823		Lack of fit	0.170	10	0.017	4.540	0.0543	
AD	5.06×10^{-4}	1	5.06×10^{-4}	0.041	0.8419		Pure error	0.018	5	3.66×10^{-3}			
BC	6.25×10^{-6}	1	6.25×10^{-6}	5.1×10^{-4}	0.9823		Total error	2.050	29				
BD	0.100	1	0.100	8.200	0.0118	*							

According to the *F*-value of the various factors, the effect of various factors on the screening loss rate in descending order of *C*, *D*, *B*, *A* within the test conditions. Furthermore, cylindrical sieve aperture and inclination angle were the main influencing factors on the screening loss rate. The analysis results of ANOVA for the response surface quadratic model were represented. A multiple-order polynomial optimum equation for screening loss rate η_L was derived as Equation (11).

$$\eta_L = 33.55 - 0.84A - 0.073B - 2.93C + 0.667D - 3.2\times10^{-3}BD + 9.6\times10^{-3}A^2 + 1.03\times10^{-3}B^2 + 0144C^2 + 0.093D^2 \quad (11)$$

The R^2 was calculated as 0.91 for the screening loss rate, indicating strong agreement between the experimental and predicted values. The *Adj*-R^2 was 0.83, as the mixture movement was random in the cylindrical sieve. The *CV* was 1.86%, suggesting that the experiment was highly reliable. The *p*-value of the "Lack of fit" was greater than 0.005, suggesting that it was not significant. The model was found to be adequate for making predictions within the range of variables employed.

Cylindrical sieve rotational speed (*A*) and cylindrical sieve diameter (*B*)

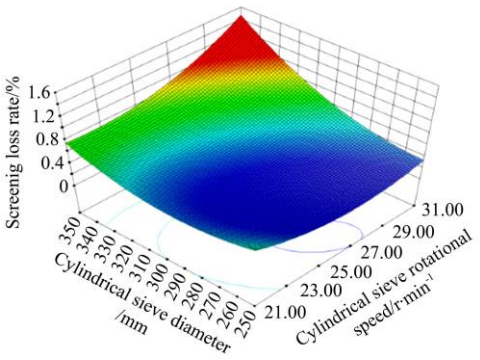

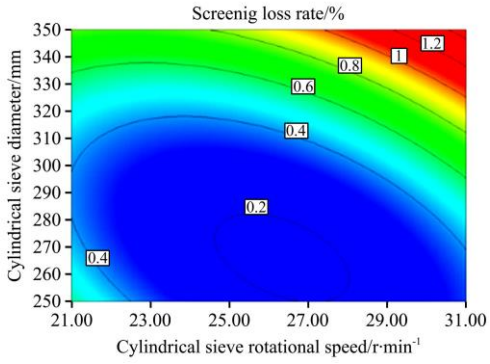

Cylindrical sieve rotational speed (*A*) and cylindrical sieve aperture (*C*)

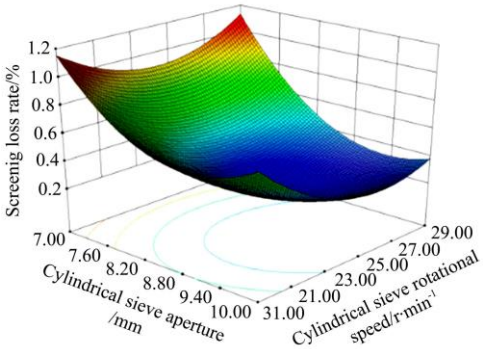

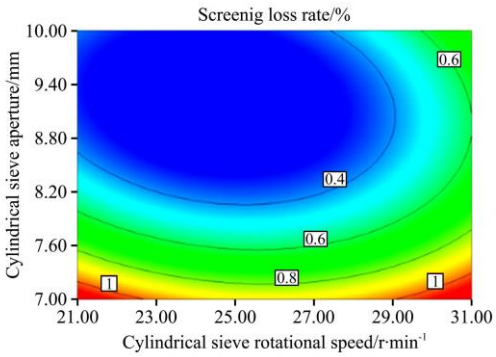

Cylindrical sieve rotational speed (*A*) and cylindrical sieve inclination angle (*D*)

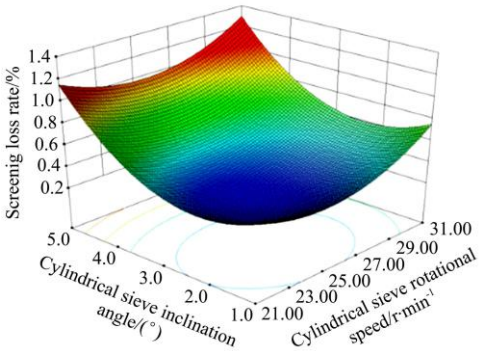

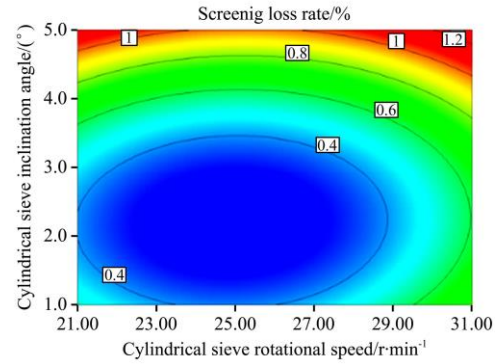

Cylindrical sieve diameter (*B*) and cylindrical sieve aperture (*C*)

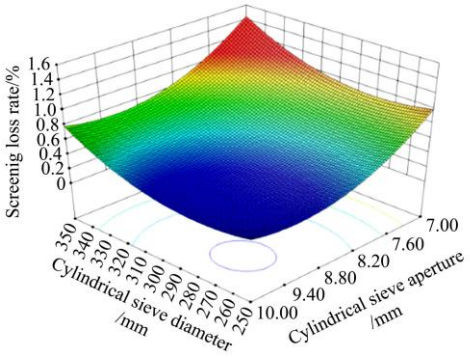

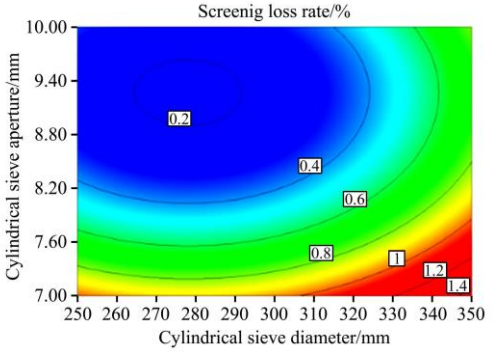

Cylindrical sieve diameter (*B*) and cylindrical sieve inclination angle (*D*)

Cylindrical sieve aperture (*C*) and cylinder inclination angle (*D*)

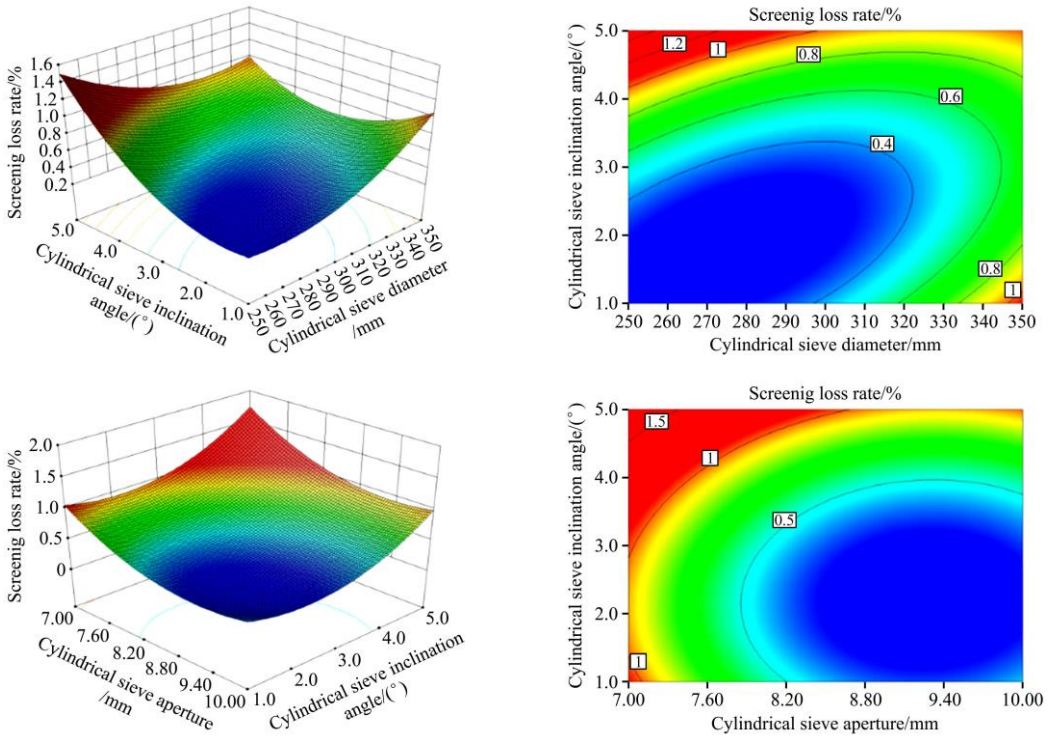

a. 3D response surface plots b. 2D contour plots

Figure 8 3D response surface plots and 2D contour plots for screening loss rate

4.2.3 CCD simulation result analysis for screening efficiency

The adequacy of the model was checked using ANOVA analysis, as shown in Table 9 and Figure 9. The *p*-value of the model was less than 0.0001, suggesting that the model was strongly significant. The *p*-value of *C* was less than 0.0001, suggesting that it was strongly significant for screening efficiency; the *p*-value of *D* was less than 0.05, suggesting that not significant for screening efficiency. The *p*-values of *A*, *B*, *AB*, *AC*, *AD*, *BC*, *BD*, and *CD* were greater than 0.05, suggesting that it was not a significant effect. According to the *F*-values of the various factors, the effects of various factors on the screening efficiency were in descending order of *C*, *D*, *A* and *B* within the test conditions.

Table 9 ANOVA for response surface quadratic model

Source	Sum of squares	df	Mean square	*F*-value	*p*-value	Significant
Model	175.63	14	12.55	12.53	<0.0001	***
A	2.98	1	2.98	2.98	0.1049	
B	0.49	1	0.49	0.49	0.4960	
C	142.59	1	142.59	142.42	<0.0001	***
D	6.89	1	6.89	6.88	0.0192	*
AB	0.30	1	0.30	0.30	0.5940	
AC	1.02	1	1.02	1.02	0.3288	
AD	0.57	1	0.57	0.57	0.4622	
BC	1.49	1	1.49	1.49	0.2416	
BD	0.89	1	0.89	0.89	0.3599	
CD	1.69	1	1.69	1.69	0.2135	
A^2	0.52	1	0.52	0.51	0.4841	
B^2	0.53	1	0.53	0.53	0.4763	
C^2	12.81	1	12.81	12.79	0.0028	**
D^2	1.82	1	1.82	1.82	0.1971	
Residual	15.02	15	1.00			
Lack of fit	13.51	10	1.35	4.48	0.0559	
Pure error	1.51	5	0.3			
Total error	190.65	29				

Furthermore, the cylindrical sieve diameter and aperture were the main influencing factors on screening efficiency. The analysis results of ANOVA for the response surface quadratic model were represented. A multiple-order polynomial optimum equation for screening efficiency η_P was derived as Equation (12).

$$\eta_P=-20.08+16.82C+2.47D-1.21C^2 \quad (12)$$

The R^2 was calculated as 0.92 for the screening cleaning rate, indicating strong agreement between the experimental and predicted values. The *Adj*-R^2 was 0.85, as the mixture movement was random in the cylindrical sieve. The CV was 1.2%, suggesting that the experiment was highly reliable. The *p*-value of the "Lack of fit" was greater than 0.005, suggesting that it was not significant. The model was found to be adequate for making predictions within the range of variables employed.

4.3 Optimization by CCD

This work used the Design-Expert software to analyze simulation results to obtain the best screening effect. The optimal conditions were as follows: the rotational speed (*A*), diameter (*B*), aperture (*C*), and inclination angle (*D*) of the cylindrical sieve were 23.6 r/min, 297 mm, 8.7 mm, and 2 °, respectively. The predicted screening cleaning rate, screening loss rate, and screening efficiency were 97.84%, 0.27%, and 85.38%, respectively.

5 Validation of the statistical model and simulation method

5.1 Validation of simulation method

The simulation method was validated using a real threshed-rice mixture and the experimental platform (Figure 5), according to the optimal parameters in Section 3.4 and the actual working conditions. The cylindrical sieve rotational speed, diameter, aperture, and inclinational angle were 23.6 r/min, 300 mm, 8.7 mm, and 2 °, respectively. The results of the simulation and three rounds of experiments are shown in Table 10.

Cylindrical sieve rotational speed (*A*) and cylindrical sieve diameter (*B*)

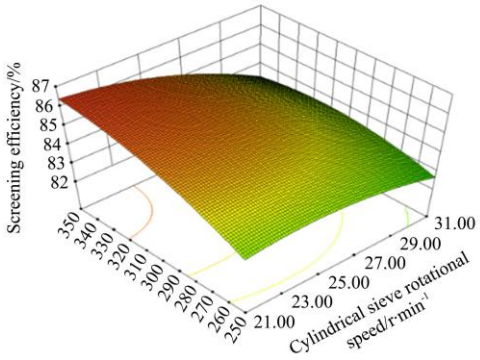

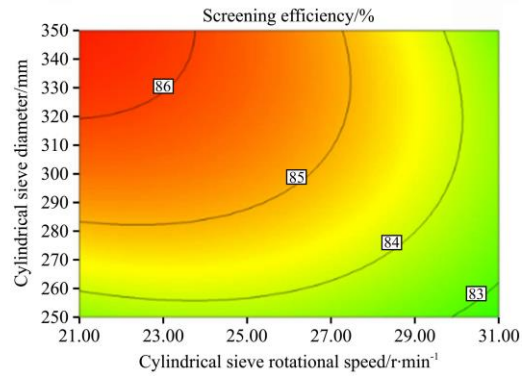

Cylindrical sieve rotational speed (*A*) and cylindrical sieve aperture (*C*)

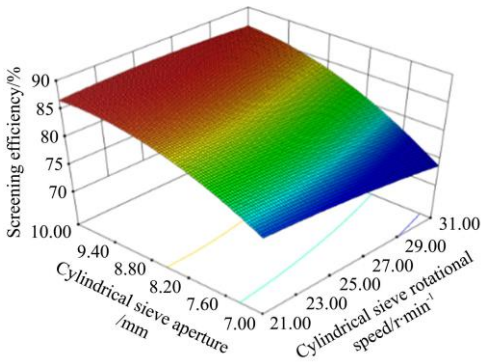

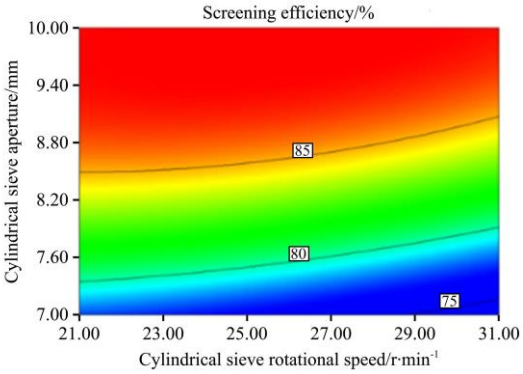

Cylindrical sieve rotational speed (*A*) and cylindrical sieve inclination angle (*D*)

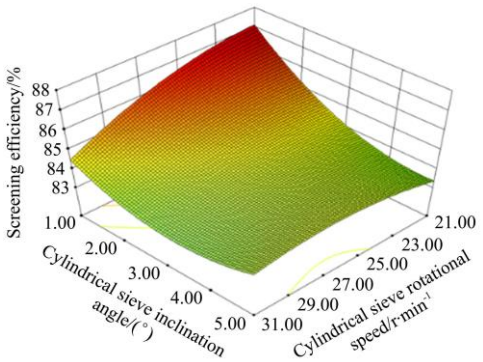

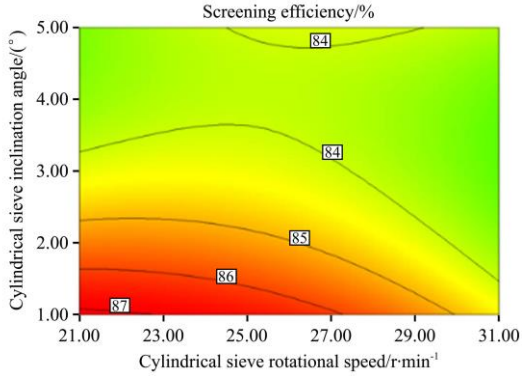

Cylindrical sieve diameter (*B*) and cylindrical sieve aperture (*C*)

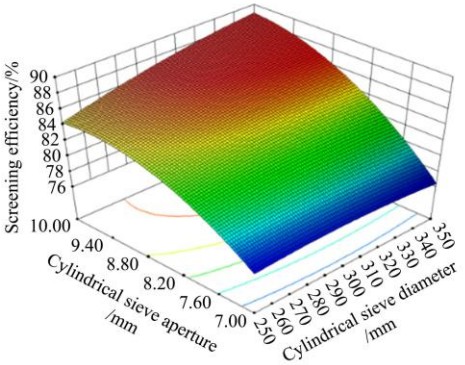

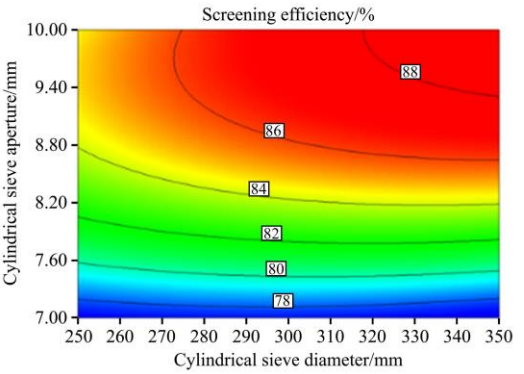

Cylindrical sieve diameter (*B*) and cylindrical sieve inclination angle (*D*)

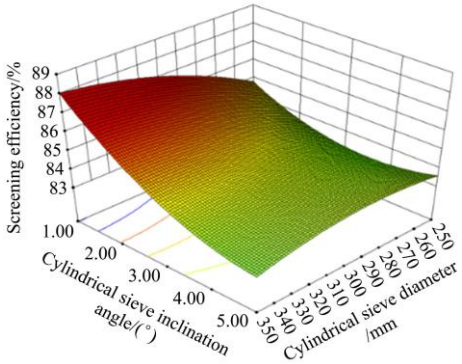

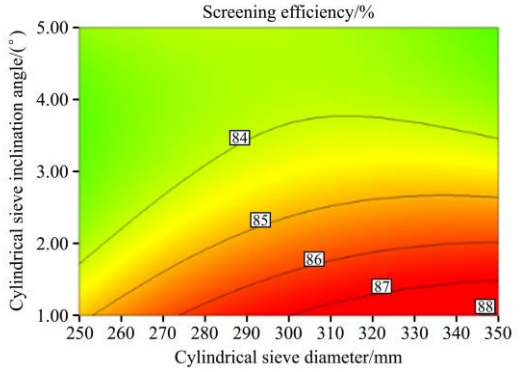

Cylindrical sieve aperture (*C*) and cylinder inclination angle (*D*)

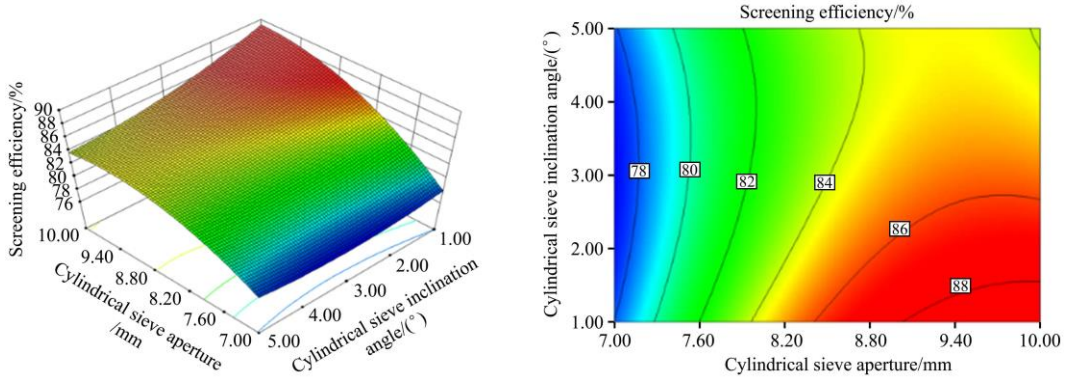

a. 3D response surface plots b. 2D contour plots

Figure 9 3D response surface plots and 2D contour plots for screening efficiency

Table 10 Comparative performance evaluation of the simulation method

Object	Screening cleaning rate of collection box/%						Screening cleaning rate/%	Screening loss rate/%	Screening efficiency/%
	1	2	3	4	5	6			
Experiment 1	99.40	96.15	96.29	96.53	95.26	95.08	96.45	0.30	83.10
Experiment 2	98.12	95.85	96.52	97.05	96.93	94.78	96.54	0.31	85.20
Experiment 3	98.30	95.45	96.72	97.85	95.53	95.52	96.56	0.32	83.83
Average value	98.61	95.82	96.51	97.14	95.91	95.13	96.52	0.31	84.04
Simulation results	100	97.45	98.06	98.49	97.65	96.98	97.88	0.28	85.31
Error/%	1.39	1.68	1.58	1.37	1.79	1.91	1.39	10.71	1.48

The experimental results were consistent with simulation with a screening cleaning rate of error within 2% in each collection box, with the rate of error for screening loss rate and screening efficiency being 10.71% and 1.48%, respectively. The screening loss rate was higher than that of the simulation due to sample loss on the conveyor belt during the experiments. The present results were close to the simulation results, and the variation trend was consistent, which further validated the reliability of this study method.

5.2 Validation of the statistical model

Validation of the statistical model was conducted by running three test simulations using mixture particle models at a fixed cylindrical sieve rotational speed of 23.6 r/min, cylindrical sieve diameter of 297 mm, cylindrical sieve aperture of 8.7 mm, and cylindrical sieve inclination angle of 2 °. The average value of simulations results for screening cleaning rate, screening loss rate, and screening efficiency were 96.58%, 0.29%, and 84.03%, respectively, and the relative errors were 1.26%, 4.94%, and 0.72%, respectively (Table 11). The test simulation results agreed with the predicted values demonstrating the validity of the statistical model.

Table 11 Comparative performance evaluation of the statistical model

Object	Screening cleaning rate/%	Screening loss rate/%	Screening efficiency/%
Simulation 1	96.60	0.28	84.80
Simulation 2	96.58	0.29	84.90
Simulation 3	96.65	0.28	84.60
Average value	96.61	0.28	84.77
Predicted results	97.84	0.27	85.38
Error/%	1.26	4.94	0.72

6 Conclusions

In this study, the DEM was utilized to simulate the separation process of grains from the mixture in a cylindrical sieve, and the main influencing factors on the screening characteristics of the mixture were analyzed. In addition, the optimal parameters were determined through CCD. The main conclusions are as follows:

1) With increases in the cylindrical sieve diameter, a decrease in the screening cleaning rate, and an increase in the screening efficiency. With increases in the cylindrical sieve aperture, a decrease in the screening cleaning rate and the screening loss rate, and an increase in the screening efficiency. With increases in the cylindrical sieve inclination angle, a decrease in the screening cleaning rate, and an obvious increase in the screening loss rate, the screening efficiency first increased and then decreased.

2) The analysis results of CCD showed that the quadratic model was very significant and was adequate for making predictions within the range of variables employed. The effect of various factors on the screening cleaning rate followed the descending order of *C*, *A*, *D* and *B*. Meanwhile, the effects of various factors on the Screening cleaning rate were in descending order of *C*, *D*, *B* and *A*. Moreover, the effects of various factors on screening efficiency were in descending order of *C*, *D*, *A* and *B*.

3) The predicted values for maximum screening cleaning rate, screening efficiency, and minimum screening loss rate were 97.84%, 0.27%, and 85.38%, respectively with the parameters *A*, *B*, *C*, and *D* being 23.6 r/min, 297 mm, 8.7 mm, and 2 °, respectively. The verification of the simulation method using real threshed rice mixture showed that the experimental results were close to the simulations, which further validates the feasibility of the simulation. Validation of the statistical model was conducted by three simulations using mixture particle models. It showed that the results agreed with the predicted values, which demonstrates the validity of the CCD under the RSM. This study details a reliable research technique and provides a design reference for cylinder sieving systems for threshed rice or separation of other bulk materials in industrial and agricultural fields.

Acknowledgements

This work was financially supported by the National Natural Science Foundation of China Youth Fund Project (Grant No. 51305182); the Ministry of Agriculture Key Laboratory of Modern Agricultural Equipment (Grant No. 201602004).

[References]

[1] Liang Y. Brief report on the forecast of world agricultural products supply and demand in 2022. World Agriculture, 2022; 3: 126–131. (in Chinese)

[2] Luo X W, Wang Z M, Zeng S, Zang Y, Yang W W, Zhang M H. Recent advances in mechanized direct seeding technology for rice. Journal of South China Agricultural University, 2019; 40(5): 1–13. (in Chinese)

[3] Bellocq B, Ruiz T, Delaplace G, Duri A, Cuq B. Screening efficiency and rolling effects of a rotating screen drum used to process wet soft agglomerates. Journal of Food Engineering, 2017; 195: 235–246.

[4] Zhang L H, Xue D Q, Ma S B, Fu C G, Hou S L. Reaserch on impurities of the cropstraw and trommel sieve. Acta Energiae Solaris Sinica, 2014; 35(3): 433–438. (in Chinese)

[5] Lyu S W, Shang S Q, Wang D W, He X N, Zhao Z L, Zhang Y D. Design and research of peanut cleaning and sorting machine. Journal of Agricultural Mechanization Research, 2019; 41(9): 71–75. (in Chinese)

[6] Wan X, Shu C, Xu Y, Yuan J, Li H, Liao Q. Design and experiment on cylinder sieve with different rotational speed in cleaning system for rape combine harvesters. Transactions of the CSAE, 2018; 34(14): 27–35. (in Chinese)

[7] Ivanov N M, Fedorenko I Y, Zakharov S E, Sukhoparov A A. Evaluating grain feed at separation by planetary cylindrical sieve with round holes. Sibirskii vestnik sel'skokhozyaistvennoi nauki, 2017; 5(47): 72–79.

[8] Sabashkin V A, Sukhoparov A A, Sinitsyn V A, Zakharov S E. Removing straw impurities from grain heaps by cylindrical sieve. Sibirskii Vestnik Sel'skokhozyaistvennoi Nauki, 2017; 47(5): 80–87.

[9] Ma Z, Li Y M, Xu L Z. Summarize of particle movements research in agricultural engineering realm. Journal of Chinese Agricultural Mechanization, 2013; 2: 22–29. (in Chinese)

[10] Grozubinsky V, Sultanovitch E, Lin I J. Efficiency of solid particle screening as a function of screen slot size, particle size, and duration of screening the theoretical approach. International Journal of Mineral Processing, 1998; 52(4): 261–272.

[11] Cheng J. Discussion on screening efficiency and hole blocking problem of circular vibrating screen. Mining machinery journal, 1988; 2: 58–61.

[12] Nati C, Magagnotti N, Spinelli R. The improvement of hog fuel by removing fines, using a trommel screen. Biomass and Bioenergy, 2015; 75: 155–160.

[13] Lau S T, Cheung W H, Kwong C K, Wan C P, Choy K K H, Leung C C, et al. Removal of batteries from solid waste using trommel separation. Waste Management, 2005; 25(10): 1004–1012.

[14] Xu S. Optimization design on trommel for sieving building sand from iron tailings. Mining & Processing Equipment, 2018; 46(1): 49–52. (in Chinese)

[15] Cundall P A. A computer model for simulating progressive, large-scale movements in blocky rock systems. In: Proceedings of Symposium of Intrnational Society of Rock Mechanics, Nancy, 1971; 1: 11–18.

[16] Ma Z, Li Y, Xu L. Discrete-element method simulation of agricultural particles' motion in variable-amplitude screen box. Computers and Electronics in Agriculture, 2015; 118: 92–99.

[17] Mustafa U, M F J, Chris S. Three-dimensional discrete element modelling of tillage: Determination of a suitable contact model and parameters for a cohesionless soil. Biosystems Engineering, 2014; 121: 105–117.

[18] Wang D, Servin M, Mickelsson K O. Outlet design optimization based on large-scale nonsmooth DEM simulation. Powder Technology, 2014; 253: 438–443.

[19] Alchikh-Sulaiman B, Alian M, Ein-Mozaffari F, Lohi A, Upreti S R. Using the discrete element method to assess the mixing of polydisperse solid particles in a rotary drum. Particuology, 2016; 25: 133–142.

[20] Ma X D, Guo B J, Li L L. Simulation and experiment study on segregation mechanism of rice from straws under horizontal vibration. Biosystems Engineering, 2019; 186: 1–13.

[21] Xu L Z, Wei C C, Liang Z W, Chai X Y, Li Y M, Liu Q. Development of rapeseed cleaning loss monitoring system and experiments in a combine harvester. Biosystems Engineering, 2019; 178: 118–130.

[22] Wang X, Zhang S, Pan H, Zheng Z, Huang Y, Zhu R. Effect of soil particle size on soil-subsoiler interactions using the discrete element method simulations. Biosystems Engineering, 2019; 182: 138–150.

[23] Lima E, Winkler E L, Tobia D, Troiani H E, Zysler R D, Agostinelli E, et al. Bimagnetic CoO Core/$CoFe_2O_4$ shell nanoparticles: Synthesis and magnetic properties. Chemistry of Materials, 2012; 24(3): 512. doi: 10.1021/cm2028959.

[24] Cundall P A, Strack O D L. A discrete numerical model for granular assemblies. Géotechnique, 1979; 1(29): 47–65.

[25] Hu G M. Analysis and simulation of granular system by discrete element method using EDEM. Wuhan: Wuhan University of Technology Press, 2010; 302p. (in Chinese)

[26] Zhou Z Y, Zhu H P, Yu A B, Wright B, Zulli P. Discrete particle simulation of gas-solid flow in a blast furnace. Computers & Chemical Engineering, 2008; 32(8): 1760–1772.

[27] Tsuji Y, Tanaka T, Ishida T. Lagrangian numerical simulation of plug flow of cohesionless particles in a horizontal pipe. Powder Technology, 1992; 71(3): 239–250.

[28] Mindlin R D. Compliance of elastic bodies in contact. Journal of Applied Mechanics, 1949; 16(3): 259–268.

[29] Li H, Qian Y, Cao P, Yin W, Dai F, Hu F, et al. Calculation method of surface shape feature of rice seed based on point cloud. Computers and Electronics in Agriculture, 2017; 142: 416–423.

[30] Yuan J B, Li H, Wu C Y, Qi X D, Shi X X, Li C. Study on apace particle modeling of rice grain basis on the Discrete Element Method. Journal of Nanjing Agricultural University, 2018; 41(6): 1151–1158. (in Chinese)

[31] Kruggel-Emden H, Rickelt S, Scherer W V. A study on the validity of the multi-sphere Discrete Element Method. Powder Technology, 2008; 188(2): 153–165.

[32] Józef H, Marek M. Parameters and contact models for DEM simulations of agricultural granular materials: A review. Biosystems Engineering, 2016; 147: 206–225.

[33] Yang S. Research of 4L-80A miniature combine harvester. Master dissertation. Nanjing: Nanjing Agricultural University, 2011; 48p. (in Chinese)

[34] Yuan J B, Wu C Y, Li H, Qi X D, Xiao X X, Shi X X. Determination and analysis of two kinds of threshed rice physical properties in South China. Journal of Agricultural Mechanization Research, 2018; 40(2): 154–159. (in Chinese)

[35] Li H C, Li Y M, Gao F, Zhao Z, Xu L Z. CFD-DEM simulation of material motion in air-and-screen cleaning device. Computers and Electronics in Agriculture, 2012; 88: 111–119.

[36] Yang X L. Study on screen-penerating performance of grains with fifferent material and shape. Master dissertation. Zhengzhou: Zhengzhou University, 2007; 84p. (in Chinese)

[37] Fang L P, Wu B L, Chan J K M, Lo I M C. Lanthanum oxide nanorods for enhanced phosphate removal from sewage: A response surface methodology study. Chemosphere, 2018; 192: 209–216.

[38] GB/T 5262-2008. Measuring method for agricultural machinery testing conditions - General rules. The Standardization Administration of China, 2008. (in Chinese)